*Key Engineering Materials*
*ISSN: 1662-9795, Vol. 542, pp 157-170*
*doi:10.4028/www.scientific.net/KEM.542.157*

*Online: 2013-02-27*

# Application of Selected Multiaxial High-cycle Fatigue Criteria to Rolling Contact Problems

Paweł Romanowicz[1,a]

[1]Cracow University of Technology, Institute of Machine Design, Cracow, Poland

[a]promek@mech.pk.edu.pl

**Keywords:** Non-proportional load, Multiaxial high-cycle fatigue, Rolling contact fatigue, Crane wheels, Roller bearings, Finite element method, Computational simulation, Contact problem.

**Abstract:** The risk of fatigue failure of elements working in rolling contact conditions (such as railway wheels, rolling bearings, etc.) is a significant issue with respect to safety and economy. In this case the complex and non-proportional stress state with pulsating three dimensional compression occurs. Therefore, the analysis of fatigue life of structures working in rolling contact conditions can be performed using recently proposed multiaxial high-cycle fatigue criteria. However, there is no hypothesis that could be universally accepted for calculations of fatigue strength. Furthermore, not all criteria proposed in literature for rolling contact fatigue (RCF) analysis can predict it. In the paper, the most popular criteria based on different theories are investigated in the application to RCF problem. Moreover, modification of the popular Dang Van hypothesis is proposed. The problem of free and tractive rolling contact fatigue is analysed on the example of a cylindrical crane wheel and spherical thrust roller bearing.

## Introduction

Rolling contact fatigue (RCF) is a localized damage process of machine elements working in rolling contact conditions produced by cyclic loading. Fatigue failure is a result of cumulative process consisting of crack nucleation, short and long crack growth and final fracture. This phenomenon is dangerous because single cycles of load would not produce any ill effects. Furthermore, the failure can occur in machine components in which the equivalent stress is below the yield point. However, in the micro scale, plastic deformation may occur in the highest stress zone during cyclic loading.

Rolling contact fatigue failure occurs in machine elements working in rolling contact conditions such as ball and roller bearing, bearing rolls, wheels and rails, cams, valves and gears. It has various forms (e.g. plastic deformations, macro or micro-pitting, spalling, crack initiation from inclusions, etc.) [1]. This type of fatigue differs from classic structural fatigue such as bending or torsional fatigue. The subsurface complex and multiaxial stresses produced by rolling contact are concentrated in a small volume of material, and so intense plastic strain can be introduced.

In the case of railway wheels three contact failure mechanisms can be considered [2, 3]:

- surface cracks, which can be initiated by plastic deformation (ratchetting),
- deep defect initiated fatigue,
- sub-surface fatigue, which typically initiates a few millimetres below the wheel tread surface.

In the process of sub-surface RCF failure the amplitudes of stresses have a dominant role. Therefore, in case of free rolling three characteristic points can be observed under the wheel tread surface [4]. One of them is the Bielajev point, in which the equivalent stress (von Mises or Tresca-Guest) achieves the highest value. In the other two points (called the Palmgren-Lundberg points), the amplitude of shear stress is the biggest. These two points are the most dangerous in repeated rolling contact.

In rolling contact concentration of stresses occurs a few millimetres below the surface [3]. In this case, the effect of non-proportional loading on fatigue life is probably similar to the case of un-notched samples. Moreover, the three dimensional pulsating compression has rather positive effect

on the fatigue. It should be noted that such character of loading is absent in classic tension-compression or bending fatigue tests. In addition cyclic three dimensional pulsating compressive stresses and shear stresses are out-of-phase. The principal axes constantly change their direction during a stress cycle. Another specific issue of this phenomenon can be found in Ref. [3]. The popular classic fatigue models (e.g. Smith, Haigh), which do not take into account the influence of non-proportional stresses at fatigue strength, cannot be applied to such analysis. Instead of this fatigue analysis of the elements mentioned above should apply multiaxial high-cycle fatigue (MHCF) hypotheses. The problem of sub-surface RCF is often investigated using Dang Van [1, 2, 5, 6, 7], Papadopoulos [2], Liu & Mahadevan [8] criteria.

A general idea of MHCF criteria is to reduce the complex, multiaxial stress state to an equivalent simple state or a damage scalar factor. They are based on different theories: critical plane in which stresses results in fatigue failure [7, 8], stress invariants as measures of fatigue load [10, 11], energy expressions estimating the fatigue strength [12], generalized extensions of empirical results [13]. All of them are clearly less universal than the hypotheses of static endurance. Generally, MHCF criteria are proposed for particular materials or specific loading conditions.

For composite materials a fuzzy set based approach in conjunction with the finite element analysis to study the variability of geometrical and mechanical parameters in the energy release rate response (the J-integral) of the cross-ply laminate [14] can be used.

Selected criteria for a particular material and/or loading (proportional or non-proportional) of calculated machine components require verification by making experiments or comparing the obtained results with other fatigue models. Therefore, if we do not have clear suggestions, it is reasonable to apply a few popular criteria and to compare their results.

**Multiaxial high-cycle fatigue criteria**

**The Sines (S) and Crossland's (C) criteria.** The criteria proposed by Sines and Crossland are among the oldest and best-known MHCF criteria and belong to the hypotheses based on stress invariants. The invariant formulae usually consist of quantities related to hydrostatic and octahedral stresses. Sines elaborated his hypothesis (Eq. 1) on the basis of the synthesis of a large number of results of fatigue tests. He assumed a linear function of the amplitude of octahedral shear stress and an average value of normal hydrostatic stress. The Sines criterion [10] can be written in the form:

$$\tau_S = \frac{1}{\sqrt{3}}\sigma_{\mathrm{vM,a}} + \left(\frac{3t_{-1}}{f_0} - \sqrt{3}\right)\cdot\sigma_{\mathrm{H,m}} \le t_{-1}, \tag{1}$$

where:

$\sqrt{J_{2,a}} = \frac{1}{\sqrt{3}}\sigma_{\mathrm{vM,a}}$ - the amplitude of second stress invariant, $\sigma_{\mathrm{vM,a}}$ - the amplitude of equivalent von Mises stress, $\sigma_{\mathrm{H,m}}$ - the mean value of hydrostatic stress, $f_0$ - repeated bending fatigue limit $\left(f_0 = \sigma_{\mathrm{a}} = \sigma_{\mathrm{m}}\right)$, $t_{-1}$ - fully reversed torsion fatigue limit $\left(\tau_a = t_{-1}, \tau_m = 0\right)$.

Application of the original Sines formula (Eq. 1) in fully reversed bending test leads to a constant ratio $t_{-1}/f_{-1} = 1/\sqrt{3}$ for all materials. This is in disagreement with experimental results for metals, which indicates that the relation $t_{-1}/f_{-1}$ changes from 0,5 for mild metals to 1,0 for brittle metals [15]. The fatigue limit $f_0$, which is seldom available, can be obtained from the Goodmann approximation:

$$f_0 = \frac{f_{-1}}{1 + \frac{f_{-1}}{\sigma_f}} \tag{2}$$

where: $f_{-1}$ - fully reversed bending fatigue limit $\left(\sigma_a = f_{-1}, \sigma_m = 0\right)$, $\sigma_{\mathrm{f}}$ - ultimate tensile strength of the material.

The Crossland criterion [11] (Eq. 3) differs from the Sines formula (Eq. 1) only in the influence of hydrostatic stress, which was assumed by Crossland with the maximal value $\sigma_{\mathrm{H,max}}$ (the first stress invariant):

$$\tau_C = \frac{1}{\sqrt{3}}\sigma_{\mathrm{vM,a}} + \left(\frac{3t_{-1}}{f_{-1}} - \sqrt{3}\right)\cdot\sigma_{\mathrm{H,max}} \le t_{-1}, \tag{3}$$

This criterion is suitable for determination of fatigue endurance in structures with predominance of torsion. One of its characteristic features is lack of hydrostatic effects for materials characterized by the relationship $t_{-1} \le \frac{\sqrt{3}}{3} f_{-1}$. The use of criteria based on stress invariants allows us to determine the initiation point of fatigue cracks. However using these criteria, the orientation of potential cracks cannot be defined.

In the RCF analysis, the amplitude of second stress invariant in the Sines method (Eq. 1) is reduced by a large mean hydrostatic compressive stress. Furthermore, the Crossland hypothesis shows much better correlations with experimental predictions than the Sines criterion [15]. Because of this, the Sines criterion cannot be recommended for multiaxial prediction of fatigue strength of element working at such conditions.

**Dang Van's criteria (DV)**

**DV criterion.** The original Dang Van hypothesis [7] is based on the mesoscopic approach of critical plane and assumes that fatigue damage appears when the load curve (which is a function of mesoscopic shear stress $\tau(t)$ and hydrostatic stress $\sigma_{\mathrm{H}}(t)$) intersects the fatigue limit domain limiting line. The Dang Van's criterion is expressed by inequality:

$$\tau_{DV}^{MAX} = \max_t\left[\tau(t) + \left(\frac{3t_{-1}}{f_{-1}} - 1{,}5\right)\cdot\sigma_{\mathrm{H}}(t)\right] \le t_{-1}, \tag{4}$$

and

$$\sigma_H(t) = \frac{1}{3}\left(\sigma_1(t) + \sigma_2(t) + \sigma_3(t)\right), \tag{5}$$

where: $\tau(t)$ – mesoscopic shear stress, $\sigma_1(t),\ \sigma_2(t), \sigma_3(t)$ – principal stresses.

**Modified Dang Van's criterion ($\mathbf{DV_{mod}}$).** In his criterion Dang Van assumes that compression effects close microcracks, which is profitable in fatigue mechanism of materials. It leads to a corresponding decrease of equivalent fatigue effort of structures working in compression conditions. In particular, it concerns hard materials. This assumption has recently been criticised [2, 5]. In application to RCF analysis a modification of the DV's criterion is proposed. In this version the hydrostatic stress effect is neglected for negative values of $\sigma_H$:

$$\tau_{DVmod}^{MAX} = \max_t\left\{\begin{array}{ll}\left[\tau(t) + \left(\frac{3t_{-1}}{f_{-1}} - 1{,}5\right)\cdot\sigma_{\mathrm{H}}(t)\right] & \text{for } \sigma_{\mathrm{H}} \ge 0\\ \tau(t) & \text{for } \sigma_{\mathrm{H}} < 0\end{array}\right\} \le \mathrm{t}_{-1} \tag{6}$$

**Papadopoulos $\mathbf{P_1}$ criterion.** The Papadopoulos $P_1$ hypothesis [15] is proposed for hard metals $\left(0{,}577 < t_{-1}/f_{-1} < 0{,}8\right)$ and is based on an average measure of resolved shear stress amplitude $\langle T_a \rangle$. The volumetric root mean square of $\langle T_a \rangle$ is equivalent to an average measure of the plastic strain

accumulated in all the flowing crystals within RVE [15]. In both Papadopoulos' presented criteria, the hydrostatic stresses $\sigma_H$ are represented by their maximal values $\sigma_{H,\max}$, similarly to the Crossland hypothesis. The $P_1$ criterion is expressed by the relationship:

$$\sqrt{\langle\langle T_a \rangle\rangle^2} + \left( \frac{3t_{-1}}{f_0} - \sqrt{3} \right) \cdot \sigma_{H,\max} \le t_{-1}, \tag{7}$$

where: $\sqrt{\langle\langle T_a \rangle\rangle^2}$ - the volumetric root mean square of resolved shear stress amplitude defined as:

$$\sqrt{\langle\langle T_a \rangle\rangle^2} = \sqrt{\frac{5}{8\pi^2} \int_{\varphi=0}^{2\pi} \int_{\theta=0}^{\pi} \int_{\chi=0}^{2\pi} \tau_a^2(\varphi,\theta,\chi) \mathrm{d}\chi \cdot \sin\theta \, \mathrm{d}\theta \, \mathrm{d}\varphi}, \tag{8}$$

$\tau_a$ - the amplitude of resolved shear stress $\tau$, appointed for fixed material plane $\Delta$ (determined by $\varphi$ and $\theta$ - Fig. 1). For a given material plane $\Delta(\varphi,\theta)$ the amplitude of resolved shear stress $\tau_a$ is a function of $\chi$:

$$\tau_a(\varphi,\theta,\chi) = \frac{1}{2}\left[ \max_{t\in T} \tau(\varphi,\theta,\chi,t) - \min_{t\in T} \tau(\varphi,\theta,\chi,t) \right], \tag{9}$$

where $T$ is a close time period considered.

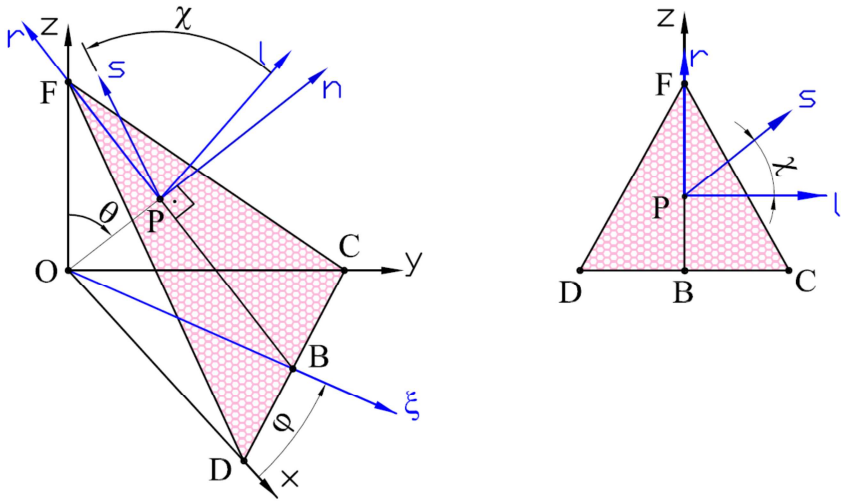


Fig. 1. Orientation of material plane $\Delta$ (CDF) crossing point O (points O and P overlap); orientation is defined by two angles: $\Delta(\varphi,\theta)$ and direction of versor ***s*** on plane $\Delta$ is defined by angle $\chi$

The $P_1$ criterion is based on integral approach. It can be indicated that the phase difference in out-of-phase bending and torsion does not have any influence on the calculated high-cycle fatigue life of a structure in such criteria. This statement is in conflict with experimental observations for particular materials [16].

**Papadopoulos 2 criterion ($P_2$).** The second Papadopoulos $P_2$ hypothesis (2001) is based on the critical plane approach [9]:

$$\tau_{P2} = \max_{\varphi,\theta}(T_a) + \left( \frac{3t_{-1}}{f_{-1}} - 1{,}5 \right) \cdot \sigma_{H,\max} \le t_{-1}, \tag{10}$$

The introduced average stress quantity denoted as $T_a(\varphi,\theta)$ is called a generalised shear stress amplitude and is calculated for each plane $\Delta$ using the formula:

$$T_a(\varphi,\theta)=\sqrt{\frac{1}{\pi}\int_{\chi=0}^{2\pi}\tau_a^2(\varphi,\theta,\chi)\mathrm{d}\chi}, \tag{11}$$

where $\tau_a$ is the amplitude (Eq. 9) of the resolved shear stress, acting on $\Delta$ along the direction defined by $\chi$.

The critical plane is defined as the plane $\Delta$ where $(T_a)$ achieves the maximal value. This criterion gives better agreement for ferritic steels with a distinct fatigue strength (endurance limit) and is proposed for multiaxial proportional and non-proportional loading [9]. Furthermore, this variant of the Papadopoulos criterion includes the effect of load phase difference at the equivalent fatigue effort.

**Lagoda energy criterion ($E_L$).** The strain energy hypothesis proposed by T. Łagoda [12] is based on the critical plane approach and distinguishes the strain energy density measure for tension and compression:

$$W_{eqv}^{MAX}=\max_t\left\{\beta\cdot W_{ns}(t)+\kappa\cdot W_n(t)\right\}\le W_{af}. \tag{12}$$

The limit ($W_{af}$) has been assumed as:

$$W_{af}=\frac{f_{-1}^2}{2\mathrm{E}}. \tag{13}$$

The position of the critical plane can be determined by observation of a certain composition of normal $W_n$ or shear $W_{ns}$ strain energy density parameter. The criterion takes into account the influence of mean strains $\varepsilon_m$:

$$W_n(t)=0{,}5\sigma_n(t)\cdot\left[\varepsilon_n(t)-\varepsilon_{n,m}\right]\cdot\mathrm{sgn}\left[\sigma_n(t),\varepsilon_n(t)-\varepsilon_{n,m}\right], \tag{14}$$

$$W_{ns}(t)=0{,}5\tau_{ns}(t)\cdot\left[\varepsilon_{ns}(t)-\varepsilon_{n,m}\right]\cdot\mathrm{sgn}\left[\tau_{ns}(t),\varepsilon_{ns}(t)-\varepsilon_{n,m}\right], \tag{15}$$

where, to distinguish tension and compression effects, function sgn(x;y) is used:

$$\mathrm{sgn}(x;y)=\frac{\mathrm{sgn}(x)+\mathrm{sgn}(y)}{2}=\begin{cases}1 & \text{gdy} \quad \mathrm{sgn(x)}=\mathrm{sgn(y)}=1\\ 0 & \text{gdy} \quad \mathrm{sgn(x)}=-\mathrm{sgn(y)}\\ -1 & \text{gdy} \quad \mathrm{sgn(x)}=\mathrm{sgn(y)}=-1\end{cases}. \tag{16}$$

In this paper, for the rolling contact fatigue calculation the presented variant $E_L$ of the criterion of the maximum parameter of shear and normal strain energy density in the plane determined by shear strain energy parameter [17] is more adequate. This version of the criterion is proposed for application to elements made of steel, steel alloys, aluminium alloys and welded alloys. It is assumed that the critical plane $\Delta$ (Fig. 1) with normal ***n*** and tangent ***s*** is determined by the maximum value of strain energy density parameter $\left(W_{ns}^{MAX}\right)$ (Eq. 15). Moreover, it is assumed that

the critical plane is determined as the mean position of one of the two planes in which $W_{ns}^{MAX}$ occurs. Material coefficients $\beta$ and $\kappa$ can be designated using pure alternating torsion and bending (or tension-compression):

$$\beta = \frac{k}{1+\nu}; \quad k = \left(\frac{f_{-1}}{t_{-1}}\right)^2; \quad \kappa = \frac{4-k}{1-\nu}, \tag{17}$$

where $\nu$ is the Poisson ratio.

There are also other versions of the energy criterion in which the critical plane is determined by different energy density parameters, but they are rather proposed for low-carbon steels, cast irons or welded steel joints [17].

**Liu & Mahadevan criterion (L&M).** The hypothesis proposed by Liu and Mahadevan is based on a critical plane concept and includes the non-linear combination of the normal stress amplitude $(\sigma_a)$, shear stress amplitude $(\tau_a)$ and hydrostatic stress amplitude $(\sigma_{H,a})$ acting on the critical plane, with formula:

$$\tau_{L\&M}^{MAX} = \sqrt{\left(\frac{\sigma_a}{f_{-1}}\right)^2 + \left(\frac{\tau_a}{t_{-1}}\right)^2 + k\left(\frac{\sigma_{H,a}}{f_{-1}}\right)^2} \le \beta, \tag{18}$$

where:

$k, \beta$ - material parameters (Table 1).

Table 1. Material parameters in L&M criterion [18]

| Material property | $s = \frac{t_{-1}}{f_{-1}} \le 1$ | $s = \frac{t_{-1}}{f_{-1}} > 1$ |
|---|---|---|
| $\alpha$ | $\cos(2\alpha) = \frac{-2+\sqrt{4-4(1/s^2-3)(5-1/s^2-4s^2)}}{2(5-1/s^2-4s^2)}$ | $\alpha = 0$ |
| $k$ | $k = 0$ | $k = 9\left(s^2-1\right)$ |
| $\beta$ | $\beta = \left[\cos^2(2\alpha)s^2 + \sin^2(2\alpha)\right]^{1/2}$ | $\beta = s$ |

In the above model, a correction factor, taking into account the mean stress effect, can also be introduced [18]. What is a characteristic feature of this criterion is that the critical plane orientation may differ from the fatigue fracture plane for different materials. The angle between the mentioned above planes $\alpha$ depends on material parameters. This makes the L&M criterion applicable in a wide range of metals from very ductile to extremely brittle. The fatigue fracture plane is assumed to be the plane in which the principal stress amplitude achieves the maximal value. A detailed description of different fatigue models based on the general formula (Eq. 18) can be found in [18].

**The problems of rolling contact fatigue of cylindrical crane wheel**

The problems of rolling contact of a cylindrical crane wheel Ø710 (Fig. 2) and crane rail A120 (rail head radius $R$ = 600 [mm]) were analysed using MHCF criteria proposed in the paper. The wheel and rail were made of 30CrNiMo8 alloy steel with material properties presented in Table 2. The vertical force $F$ = 294,3 [kN] loading the crane wheel with maximal admissible design value [19] was adopted in fatigue calculation. The initial contact point in free and tractive rolling contact was assumed to occur at the centre of the crane wheel and rail.

In both cases, the sub-surface fatigue is one of the contact failure mechanisms [2, 3]. The sub-surface cracks typically nucleate a few millimetres below the wheel thread surface where the largest shear stress occur. With the increase of speeds and axle-loads (in particular railway wheels) the fatigue has larger influence on decrease of the durability and safety of the whole structure. Therefore, a better prediction of fatigue life is an important issue. This failure mechanism is often investigated using MHCF criteria [1-3, 5-8]. In the rolling contact, the sub-surface stresses generated by a moving contact are complex and non-proportional and depend on different parameters such as: type of contact, friction, creep forces. The influence of different parameters on fatigue of railway wheels and rails is described in [3].

Two kinds of rolling contact were investigated. First – free rolling (frictionless) for steady motion and second – tractive rolling. Both problems of three dimensional contact were solved using the finite element method (ANSYS®).

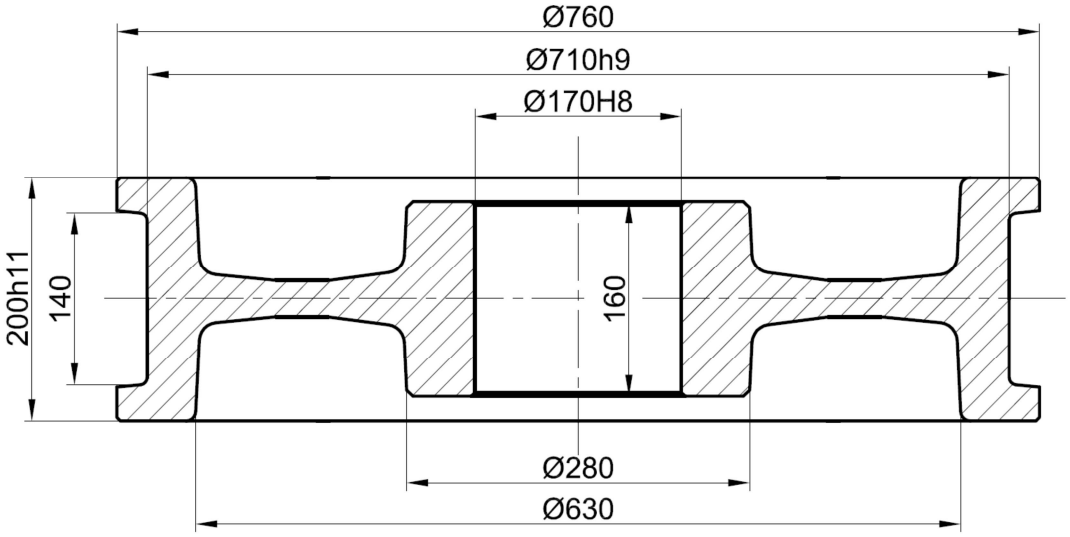


Fig. 2. Cross-section and main dimensions of the cylindrical crane wheel Ø710

Table 2. Material properties of 30CrNiMo8 steel [20]

| Parameter | $f_{-1}$ | $t_{-1}$ | $\sigma_y$ (yield limit) | $\sigma_f$ (tensile strength) |
|---|---|---|---|---|
| Value [MPa] | 549 | 370 | 1050 | 1250 |

**Free (frictionless) and tractive rolling contact fatigue of cylindrical crane wheel.** In the free rolling case sliding and spin do not occur, also friction effects are very small and can be neglected. Obviously, the calculations using the 3D finite element method (FEM) are more appropriate due to complex geometry of real objects. The element mesh in the numerical model (Fig. 3a) was irregular with strong concentration of hexahedrons in the contact area. The structural 3D solid 20-node elements SOLID95, 3D surface to surface 8-node contact elements CONTA174 and 3D target 8-node elements TARGE170 were used in the calculations. To increase computational efficiency and accuracy submodelling technique was used.

In the case of driving wheels (tractive rolling contact) it is necessary to include the traction effect between wheel and rail. In order to perform this analysis, modification of rail A120 model was proposed. For this purpose, a new part with small stiffness ($E_2$ = 500 [MPa]) was added at the bottom of the rail in the numerical model (Fig. 3b). This added part was not included in the free rolling contact calculations. It allows small translation under tractive force and allows getting a correct form of the stiffness matrix. Also, the friction coefficient $\mu$ = 0,15 between wheel and rail and torque moment $M$ = 14,4 [kNm] driving the wheel (almost equal to its critical value for $\mu$ = 0,15) were taken into account unlike in the numerical model for the free rolling contact.

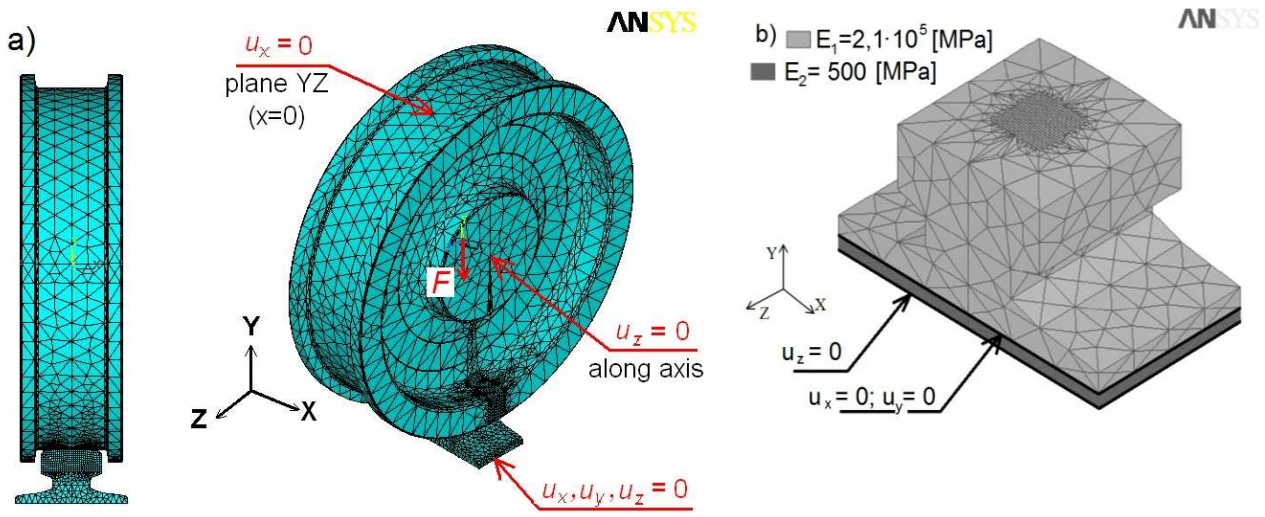


Fig. 3. 3D-model of free rolling contact of crane wheel with rail for free (a) and tractive rolling contact (b)

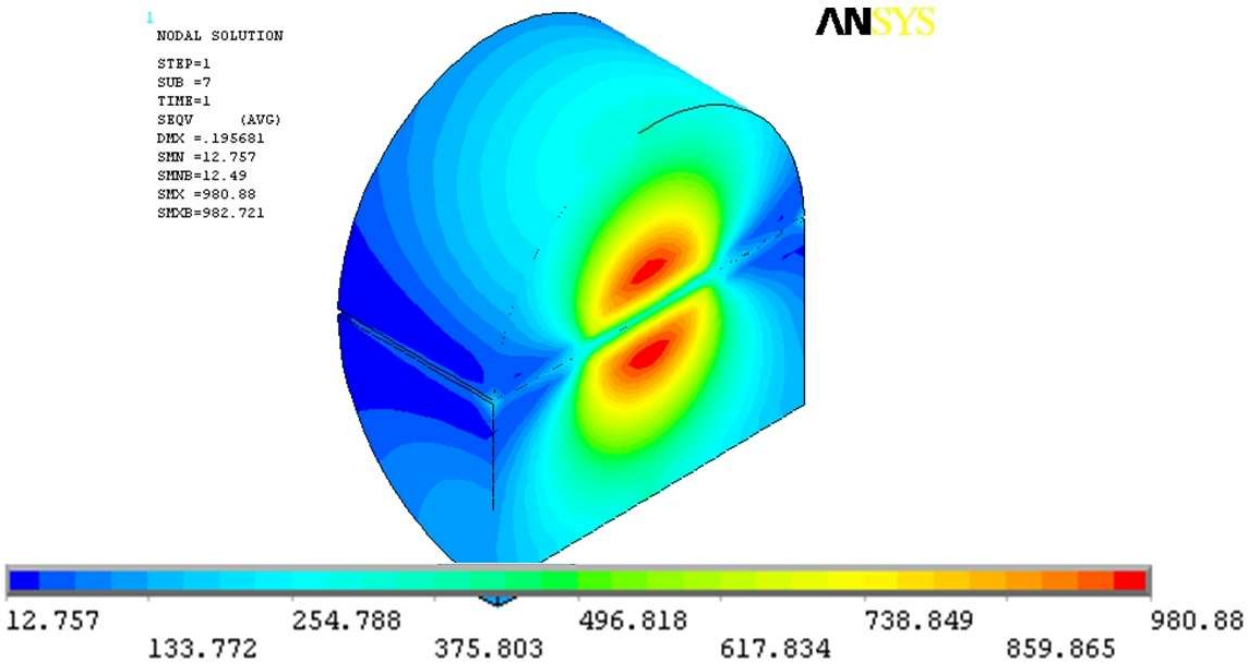


Fig. 4. Von Mises stress distribution at the cross section of the crane wheel and rail below the contact area in free rolling contact

The obtained numerical results of maximal contact stresses for free rolling were compared with the theoretical solution [4]. The results of the sub-model solution are presented in Fig. 4 and Fig. 5. Fig. 4 shows the equivalent Von Mises stress in YZ-plane. The maximum value of the Von Mises stress occurs at 4,5 millimetres below the wheel tread surface in the Bielajev point. It can be observed that high stresses only occur within a small volume above the contact area. The maximum shear stress amplitude occurs on the radius of Palmgren-Lundberg points at a depth of about 3 [mm] below the wheel tread surface. For frictionless rolling contact, the "butterfly" distribution of shear stress $\tau_{yz}$ can be observed (Fig. 5).

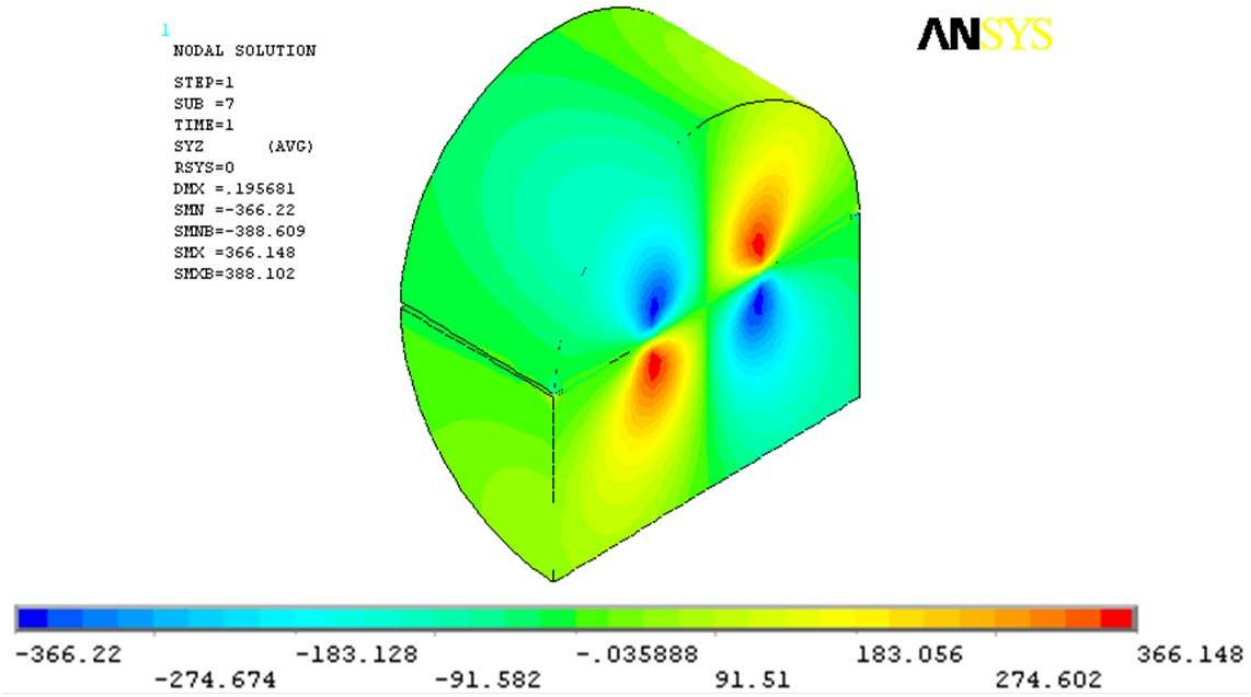


Fig. 5. Shear stress distribution at the cross section of the crane wheel and rail below the contact area in free rolling contact

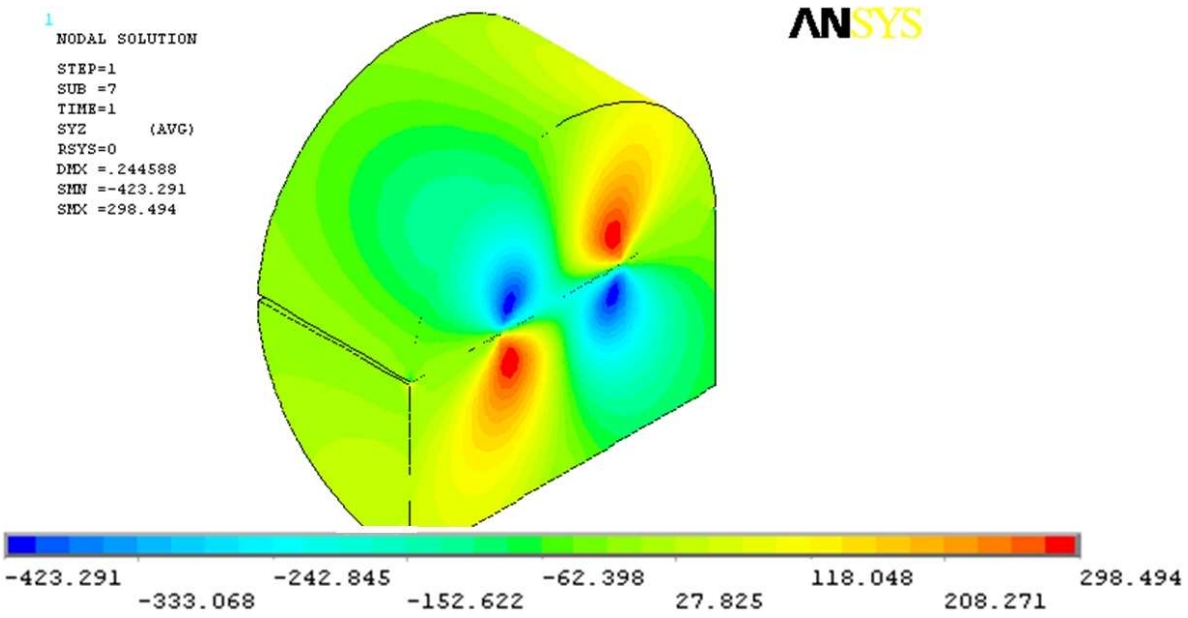


Fig.6. Shear stress distribution at the cross section of the crane wheel below the contact area in tractive rolling contact

Including traction effect leads to a distortion of the characteristic anti-symmetric shear stress distribution. The absolute values of the maximal and the minimal $\tau_{yz}$ shear stresses are different (Fig. 6). Another significant difference is that the tension effect occurs at one end of the contact area. Consequently, the possibility of surface cracks should be investigated for larger friction coefficient and surface roughness [4].

**The analysis of spherical thrust roller bearing**

Ball and roller bearings are among the most important machine elements. Due to the cyclical contact stresses, elements of rolling bearings are subjected to the rolling contact fatigue phenomena [21]. Generally, fatigue cracks appear immediately below the load carrying surface where the largest shear stress amplitude occurs. However, they can initiate at the surface and grow from there into the material. Finally, after a certain number of cycles, cracks extend up to the surface and fragments of material break away. This phenomenon (known as pitting or spalling) progressively increases and eventually makes the bearing unserviceable.

For standard load, the fatigue life of rolling bearing ($L$ – the fatigue life in revolutions $\cdot 10^6$) can be predicted using relationship developed by Palmgren & Lundberg [22]:

$$L = \left(\frac{C}{P}\right)^k, \tag{19}$$

where: $C$ - basic (dynamic) load rating, $P$ – selected load, $k$ – exponent of the life equation (for linear contact $k = 10/3$).

The predicted life from the above equation is based on experimental test of rolling bearings analysed statistically. Another probabilistic engineering and deterministic research models which can be adopted for fatigue life calculation of rolling bearings are presented and discussed in [22]. Most of them are based on certain assumption and/or have some limitations. Moreover, application of the above models (in particular – engineering models; e.g. P&L (Eq. 19)) may require expensive and time consuming RCF endurance testing.

Application of MHCF criteria in the analysis of subsurface crack initiation in such problems seems to be reasonable. Such criteria require only popular fatigue tests (fully reversed bending and torsion) for investigated material and can be easily adopted to fatigue life analysis of roller bearings.

The fatigue analyses were performed for a spherical thrust roller bearing designated as 293/1600 EF [23]. This bearing is perfectly suited for heavy duty applications with axial loads or combined axial and radial loadings. They are frequently used in industries such as metalworking, plastics, marine, industrial gearboxes, material handling, mining and constructions. The most important information on the investigated roller bearing is presented in Table 3.

Table 3. Dimensions and load ratings of investigated spherical thrust roller bearing [23]

| Designation | Principal dimensions | | | Basic load ratings | | Fatigue load limit |
|---|---|---|---|---|---|---|
| | | | | dynamic | static | |
| | $d$ | $D$ | $H$ | $C$ | $C_0$ | $F_u$ |
| | [mm] | | | [kN] | | [kN] |
| 293/1600EF | 1600 | 2280 | 408 | 36800 | 200000 | 11800 |

**Numerical model**

In order to perform fatigue analysis, it was assumed that both rings and rolling elements are made from the same material X105CrMo17. Some material properties of this stainless steel with high chromium content are given in Table. 4. The values of the fully reversed bending and torsion fatigue limit were estimated on the basis of tensile strength ($\sigma_f$). The detailed information on rolling bearings is not provided by manufacturers. For this reason, a one-point contact between rolling element and rings was assumed in the numerical model. The calculations were performed for different contact conditions with various radii of spherical roller element contact surface - $R_{Bar}$. The radius of inner and outer rings contact surfaces was $R_p$ = 1580 [mm]. Two most interesting examples for $R_{Bar}$ = {1545; 1560} [mm] have been presented in the paper.

Table 4. Material properties of steel X105CrMo17 after heat-treatment [24]

| Parameter | $E$ | $\sigma_y$ | $\sigma_f$ | Hardness | $f_{-1}$ | $t_{-1}$ |
|---|---|---|---|---|---|---|
| Value | $2{,}23 \cdot 10^5$ [MPa] | 1635 [MPa] | 1780 [MPa] | 56 [HRC] | $0{,}4 \cdot R_m = 712$ [MPa] | $0{,}6 \cdot Z_{GO} = 427$ [MPa] |

The calculations of subsurface stresses were performed using finite element method (ANSYS®). The structural high-order 3D solid (SOLID95) and contact elements (CONTA174) were used in the calculations. Furthermore, the rolling friction coefficient $\mu = 0{,}0018$ was adopted in the investigated model. The axial load $F_a$ equal to the fatigue load limit $F_u$ =11800 [kN] suggested by the producer [23] was adopted. Due to the symmetry, only a half part of rolling element was modelled (Fig. 7). The detailed analysis (e.g. engineering application, contact and subsurface stress distribution analysis) of the presented spherical thrust roller bearing is presented and discussed in Ref. [25].

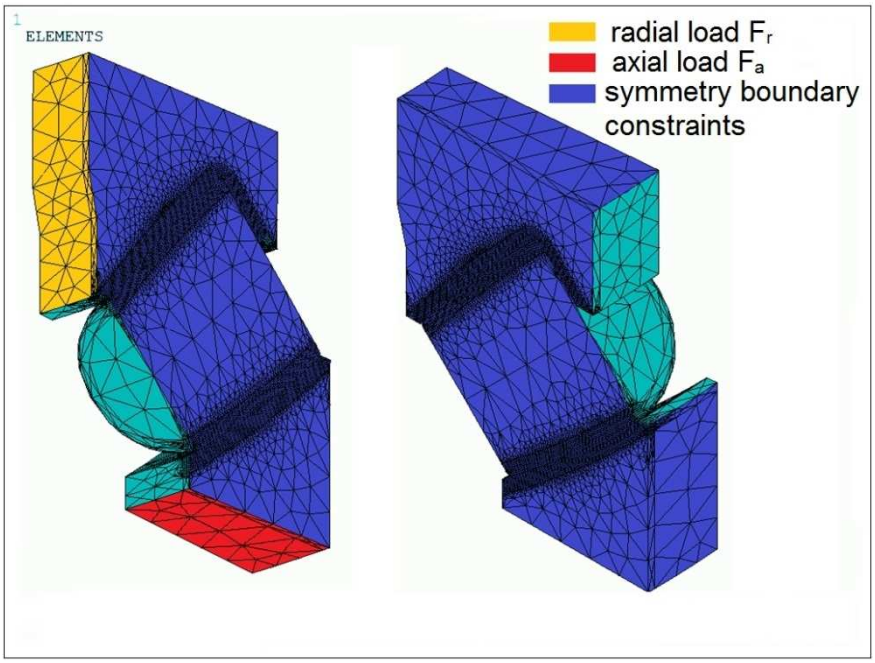


Fig. 7. Numerical model of spherical thrust roller bearing

**Results**

The fatigue analyses of the crane wheel and the spherical thrust roller bearing were performed using the presented MHCF criteria. Verification of the criteria for different materials (i.e. hard steel, mild steel, cast iron, 30CrMiNo8 steel) and loading conditions (i.e. in-phase and out-of-phase bending plus torsion loading) can be found in [2, 4, 9, 15, 18]. The safety factor was calculated in relation to the admissible value of equivalent fatigue stress with formula:

$$x_z = \frac{\text{right hand side of criterion}}{\text{maximal value of left hand side of criterion}}. \tag{20}$$

In all the investigated examples, the maximal fatigue effort occurs a few millimetres below the contact area. Almost all described criteria indicate fatigue failure of the investigated crane wheel for proposed loading ($x_z < 1$ in Table 5). However, in most cases ($P_2$, $DV_{mod}$, C, $E_L$, L&M criteria) the adopted load $F$ = 294,3 [kN] is close to its critical value. Also, it can be observed that the wheels with traction moment are more exposed to fatigue failure.

In the second investigated case of spherical thrust roller bearing, the $P_1$ hypothesis gave the closest solution to the admissible fatigue load limit suggested by the producer. However, the fatigue life $L$ calculated using P&L relationship (Eq. 19) is about 40 million revolutions for this loading, while rating life $L_{10}$ for rolling bearings is 10 million revolutions. On the other hand, the fatigue life for the maximal admissible fatigue loading calculated using the remaining criteria ($DV_{mod}$, $P_2$, $E_L$) was between $L = 10 \div 13 \cdot 10^6$ revolutions [25].

Table 5. The estimated values of the fatigue safety factor $x_z$ in the cylindrical crane wheel in the case of free and tractive rolling contact (material 30CrNiMo8) and the spherical thrust roller bearing (material X105CrMo17)

| Criterion | Crane wheel (frictionless model) | Crane wheel (model with traction) | Spherical thrust roller bearing $R_{Bar}$ = 1560 [mm] | Spherical thrust roller bearing $R_{Bar}$ = 1545 [mm] |
|---|---|---|---|---|
| Original Dang Van (DV) | 1,57 | 1,53 | 1,83 | 1,69 |
| Modified DV ($DV_{mod}$) | 1,01 | 1,03 | 1,29 | 1,16 |
| $P_1$ | 0,79 | 0,78 | 1,04 | 0,98 |
| $P_2$ | 0,99 | 0,99 | 1,30 | 1,16 |
| C | 0,96 | 0,93 | 1,14 | 1,09 |
| $E_L$ | 0,98 | 0,94 | 1,26 | 1,14 |
| L&M | 0,98 | 0,95 | 1,31 | 1,20 |

**Concluding remarks**

Using the proposed MHCF criteria for rolling contact problems it can be found that the application of such criteria allows us to determine the safety factor, or in many cases, the fatigue life prediction. However, the performed calculations show that not all the criteria are applicable in RCF. The results obtained using DV and $P_1$ hypotheses significantly differ from the others.

The criteria based on the integral approach (such as Papadopoulos 1) give the most conservative results in the rolling contact analysis. Overestimation of the fatigue effort in relation to other criteria is caused by not taking into account the effect of shift in phase between the normal and shear stresses, which is very significant in such problems. This result confirms with the experimental tests for the notched specimens. However, in the case of rolling contact the concentration of stresses is not caused by a notch and cracks initiation below the surface. Therefore, the results obtained using $P_1$ criterion may be overestimated due to neglecting the shift in phase between stresses.

On the other hand, in the Sines and original Dang Van hypotheses shear stress amplitude is reduced by a large compressive stress. It results in underestimation of the equivalent fatigue effort of elements working in rolling contact conditions. This effect has recently been criticised in several papers [2, 5, 26] suggesting that the original DV formula should not be applied to the rolling contact fatigue problems. Therefore, a modification of the original Dang Van formula was proposed and verified in the present paper.

The proposed modified Dang Van model ($DV_{mod}$) and other investigated criteria based on different approaches (critical plane – $P_2$ and L&M, energy with critical plane – $E_L$, stress invariants – C) gave similar results in both cases. Furthermore, the results obtained using above criteria was in good agreement with fatigue load limits proposed by manufacturers for both investigated problems.

It can be concluded that the equivalent fatigue effort is somewhere inside the indicated range. However, in the author opinion, to determine the influence of three-dimensional compression with non-proportional shear on the subsurface fatigue, special tests including this kind of loading should be performed. Hence, if there are no experimental tests including the stress state in elements working in rolling contact conditions, it is reasonable to use criteria based on integral approach such as $P_1$, which gives the most conservative results.

**References**

[1] Ciavarella M., Monno F., Demelio G., On the Dang Van fatigue limit in rolling contact fatigue, International Journal of Fatigue 28 (2006) 852–863.

[2] Bernasconi A., Filippini M., Foletti S., Vaudo D., Multiaxial fatigue of a railway steel under non-proportional loading, International Journal of Fatigue 28 (2006) 663–672.

[3] Ekberg A., Kabo E., Fatigue of railway wheels and rails under rolling contact and thermal loading – an overview, Wear 258 (2005) 1288–1300.

[4] Romanowicz P., Fatigue analysis of selected machine elements working at rolling contact condition, PhD Thesis, Cracow University of Technology, Cracow 2010.

[5] Desimone H., Bernasconi A., Beretta S., On the application of Dang Van criterion to rolling contact fatigue, Wear 260 (2006) 567–572.

[6] Ekberg A., Rolling contact fatigue of railway wheels – a parametric study, Wear 211 (1997) 280-288.

[7] Dang Van K., Maitournam M. H., On some recent trends in modelling of contact fatigue and wear in rail, Wear 253 (2002) 219–227.

[8] Liu Y., Stratman B., Mahadevan S., Fatigue crack initiation life prediction of railroad wheels, International Journal of Fatigue 28 (2006) 747–756.

[9] Papadopoulos I.V., Long life fatigue under multiaxial loading, International Journal of Fatigue 23 (2001) 839–849.

[10] Sines G., Behaviour of metals under complex static and alternating stresses, in: Metal Fatigue, McGraw Hill, New York, 1959, 145-169.

[11] Crossland B., Effect of large hydrostatic pressures on the torsional fatigue strength of an alloy steel, Proc. Int. Conf. Fatigue of Metals, London, 1956, pp. 138–49.

[12] Łagoda T., Energy models for fatigue life estimation under uniaxial random loading. Part I: The model elaboration, International Journal of Fatigue 23 (2001) 467–480.

[13] Weber B., Fatigue multiaxiale des structures industrielles sous chargement quelconque [En ligne] Thèse : Institut National des Sciences Appliquées de Lyon, 1999.

[14] Muc A., Kędziora P., A fuzzy set analysis for a fracture and fatigue damage response of composite materials, Compos. Str. 54 (2001) 283-287.

[15] Papadopoulos I.V., Davoli P., Gorla C., Filippini M., Bernasconi A., A comparative study of multiaxial high-cycle fatigue criteria for metals, International Journal of Fatigue vol.19 no. 3 (1997) 219-235.

[16] Bong-Ryul You, Sonn-Bok Lee, A critical review on multiaxial fatigue assessments of metals, International Journal of Fatigue, vol. 18 № 4 (1996) 235-244.

[17] Kluger K., Łagoda T., Wpływ wartości średniej obciążenia na trwałość zmęczeniową w opisie energetycznym. Wieloosiowe zmęczenie losowe elementów maszyn i konstrukcji - część XI, Politechnika Opolska, Opole, 2007.

[18] Liu Y., Mahadevan S., Multiaxial high-cycle fatigue criterion and life prediction for metals, International Journal of Fatigue 27 (2005) 790–800.

[19] Information on http://www.demagcranes.pl.

[20] Esderts A., Betriesfestigkeit bei mehrachsiger Biege- und Torsionbeanspruchung, Technische Universitat Clausthal, 1995.

[21] SKF, Bearing failures and their causes, 1994, information on http://www.skf.com.

[22] Sadeghi F., Jalalahmadi B., Slack T. S., Raje N., Arakere N. K., A Review of Rolling Contact Fatigue, Journal of Tribology 131 (2009) 041403 1-15.

[23] Information on http://www.skf.com.

[24] Information on http://www.interlloy.com.au/data_sheets/stainless_steel/440c.html.

[25] Romanowicz P., High-cycle fatigue analysis of spherical roller bearing: submitted to Przegląd Mechaniczny (2012).

[26] Papuga J., A survey on evaluating the fatigue limit under multiaxial loading, International Journal of Fatigue 33 (2011) 153–165.